Journal of Structural Geology, Vol. 11, No. 3, pp. 255 to 273, 1989
Printed in Great Britain

0191-8141/89 $03.00 + 0.00
© 1989 Pergamon Press plc

Regional, structural and strain analyses of terranes in the Western Metamorphic Belt, Central Sierra Nevada, California

SCOTT R. PATERSON, OTHMAR T. TOBISCH and TAPAS BHATTACHARYYA*

Earth Science Board, University of California at Santa Cruz, Santa Cruz, CA 95064, U.S.A.

(*Received* 23 *November* 1987; *accepted in revised form* 10 *August* 1988)

Abstract—A comparison of total strains in 225 samples from the Western Metamorphic Belt, Sierra Nevada, shows that strain types and intensities strongly depend on rock type. Greywackes and clast-supported conglomerates are least strained, whereas more intense strains occur in lapilli tuffs, pebbly mudstones and slates. Large belts of volcanic rock record plane strain whereas nearby slate and greywacke sequences record flattening-type strain suggesting that volume losses of 45–65% occurred in slates and 0–26% in greywackes. Lapilli tuffs record less than 11% volume loss. The differences in volume loss and strain from one rock type to another require that discontinuities in total strain occur at most lithologic contacts.

Independently of the lithologic control, regional structural patterns and strain fields support the delineation of three terranes (Foothills, Merced River and Northern Sierra) and two distinct domains (western and eastern Foothills terranes) at these latitudes within the Western Metamorphic Belt. These terranes, each bordered by large ductile shear zones, differ in average strain intensity and orientation but not in strain type. In the Foothills terrane strain intensities decrease from moderate values in the western Foothills terrane to low values in the eastern Foothills terrane. Strain intensities in the study area are highest in the Melones and Bear Mountains fault zones and in terranes east of the Melones Fault.

Structures associated with regional deformation in each terrane do not extend far across terrane boundaries; multiple generations of regionally developed structures are, therefore, rare in this part of the Western Metamorphic Belt. Outside of fault zones, we see one regionally developed cleavage in the Foothills terrane, a single but older cleavage in the Merced River terrane and two still older cleavages in the Northern Sierra terrane. However, younger deformations may have reactivated and rotated older structures in adjacent terranes. The timing and kinematics of the deformation in the Foothills terrane suggest that faulting and rigid-body rotations preceded pervasive shortening, continued fault movement and rotation of faults to steep dips. If orientations of ductile structures reflect plate motions, structures in the Merced River terrane suggest Jurassic–Triassic orthogonal NNE convergence, whereas structures in the Foothills terrane support late Jurassic orthogonal NE convergence changing to oblique ENE convergence about 150 Ma ago.

INTRODUCTION

RECENT tectonic models suggest that the Western Metamorphic Belt, Sierra Nevada (Fig. 1) consists of numerous fault-bounded terranes (Saleeby 1981, Schweickert 1981, Blake *et al.* 1982, Nokleberg 1983). If so, each terrane should presumably display a unique set of structures and associated strain fields. These structures, as well as structures in the bounding faults, provide clues as to how the terranes were accreted and subsequently deformed. The present study examines total and some incremental strain data and related structures in a region extending across southern portions of the Western Metamorphic Belt (Fig. 2). We have used the structural/strain data to address the following question. (1) What is the extent and structural character of different terranes in this portion of the Western Metamorphic Belt? (2) How do the strain fields vary within and between these terranes? (3) What are the characteristics of the bounding faults? (4) What do the structural/strain patterns tell us about the kinematics of terrane amalgamation and deformation?

An expected result of this study (Cobbold 1977, Ramsay 1982, Treagus 1983), but one that is sometimes glossed over in regional syntheses, is that most rock types behave differently during deformation, resulting in different intensities, types and orientations of strains and related structures. Our data indicate that most lithologic contacts represent some form of strain discontinuity which often, along with the intervening domains, record unique deformational histories. Once this lithologic control is fully taken into account, regional structural/strain patterns can still be recognized and used to address the questions outlined above.

STRUCTURAL ANALYSES

Regional framework

The Sierra Nevada is divided into a series of eastern roof pendants of continental platform and volcanic arc affinities, a central Jurassic–Cretaceous batholith, and a western region dominated by oceanic metavolcanic and metasedimentary rocks called the Western Metamorphic Belt (Fig. 1, inset). Southern portions of the Western Metamorphic Belt have been divided into four fault-bounded terranes (Fig. 1): (1) the Foothills terrane consisting of metamorphosed volcanic, sedimentary and ocean-floor assemblages west of the Melones fault zone: (2) the Sullivan Creek terrane or greenschist–phyllite

* Present address: Department of Geology and Geophysics, University of Allahabad, Allahabad 211002, India.

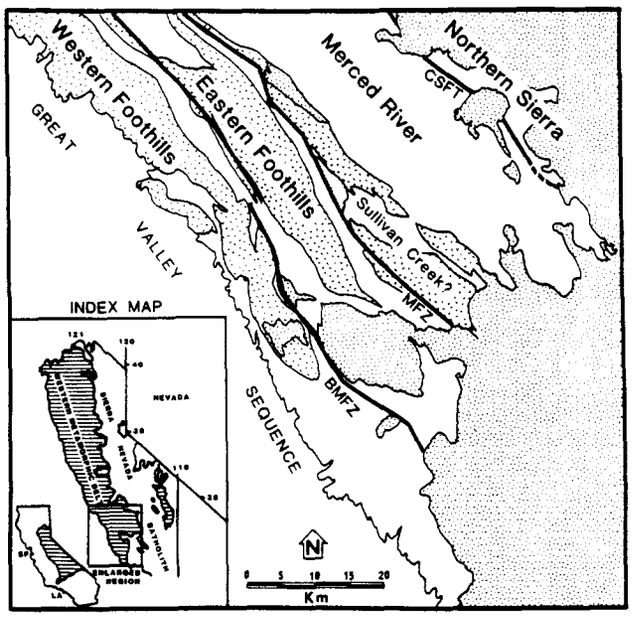

Fig. 1. Map outlining portions of the Western Metamorphic Belt, Sierra Nevada, California, examined during the present study. Random v pattern = volcanic rocks; random dash pattern = plutonic rocks; wavy line pattern = ultramafic rocks; and no pattern = metasedimentary rocks (or the non-metamorphosed Cretaceous Great Valley Sequence). The results from this study suggest that the Bear Mountains (BMFZ), Melones (MFZ) and Calaveras–Shoo Fly (CSFT) faults, represent important structural/strain discontinuities in this area. These faults mark the borders of the Northern Sierra, Merced River, and eastern and western Foothills terranes. The existence and interpretation of a fourth terrane, the Sullivan Creek terrane, is controversial and discussed in the text. Index map shows location of the figure in California.

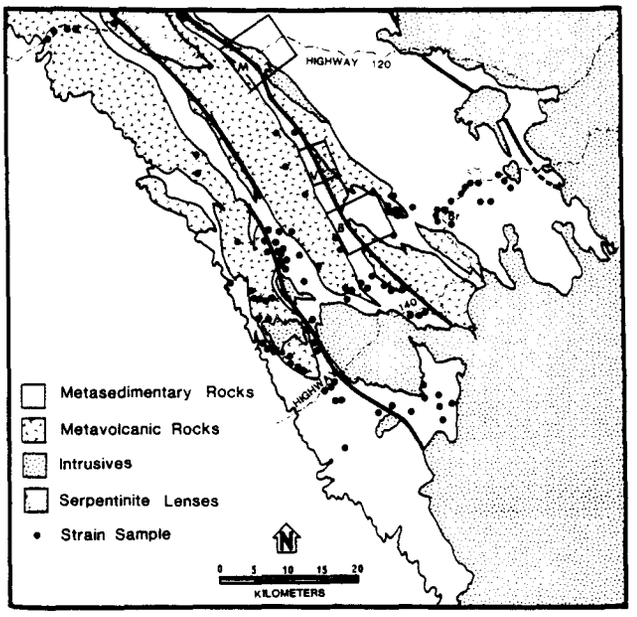

Fig. 2. Same area as Fig. 1 showing regions of detailed strain analyses near Moccasin (M), Virginia Mines (V) and Bagby (B), California, outlined with large boxes. Sample locations too closely spaced in these boxes to show at scale of this figure. Locations of strain samples analyzed outside of these boxes are shown as large dots. Domains in which bulk strains were calculated (see text and Tables 1–4) include the western and central Foothills terrane (see Fig. 1), the Moccasin, Virginia Mines and Bagby domains in the eastern Foothills and Sullivan Creek terranes, and the Moccasin and Briceburg (Br) regions in the Merced River terranes. Patterns the same as in Fig. 1.

belt consisting of volcanic rock and surrounding phyllites immediately east of the Melones Fault; (3) the Merced River terrane or Calaveras complex dominated by phyllites and cherts east of the Sullivan Creek terrane and west of the Calaveras–Shoo Fly Fault; and (4) the Northern Sierra terrane or Shoo Fly complex consisting of quartzites, marbles and phyllite located east of the Calaveras–Shoo Fly Fault (Schweickert *et al.* 1977, Saleeby 1981, 1982, Blake *et al.* 1982, Merguerian 1982, Nokleberg 1983, Schweickert & Bogen 1983, Bateman *et al.* 1985, Sharp 1988). The Foothills terrane is separated into western and eastern zones by a third major fault, the Bear Mountains fault zone (Clark 1960, Paterson *et al.* 1987a).

Some uncertainty surrounds the nature of the contact between the Sullivan Creek and Merced River terranes. Schweickert & Bogen (1983) have suggested that the Sullivan Creek terrane is part of the Foothills terrane and that this terrane is separated from the Merced River terrane by the Sonora Fault, a suture suggested to be of late Jurassic age. This interpretation has been questioned by Bateman *et al.* (1985), Bhattacharyya & Paterson (1985) and Sharp (1985) who see no structural evidence for a late Jurassic fault zone separating the Sullivan Creek and Merced River terranes in southern portions of the Western Metamorphic Belt. A zone of shearing does occur along the contact between volcanic and metasedimentary rocks near Briceburg, California (Fig. 2), which is west of the region originally proposed for the Sonora Fault (Bhattacharyya & Paterson 1985; Schweickert *et al.* 1985) However, the continuity of pre-late Jurassic rock types, structures and strains across this contact, and the occurrence of such shear zones along most volcanic–metasediment contacts in the Western Metamorphic Belt, suggest that this shear zone is not a late Jurassic suture. However, because of the uncertainty surrounding this region, we will present the geology of these two terranes separately in order to examine the nature of this boundary more thoroughly.

In the region examined, we recognize two prominent structural breaks, the Melones and Calaveras–Shoo Fly faults. Units west of the Melones Fault are all characterized by a NW-striking cleavage until recently considered by most workers to be late Jurassic (Fig. 3, Clark 1964, Schweickert *et al.* 1984), but now shown to be early Cretaceous in southwestern portions of the Foothills terrane (Paterson *et al.* 1987b, Tobisch *et al.* in press). Units between the Melones and Calaveras–Shoo Fly faults contain an older and usually more intensely developed WNW–NW-striking continuous cleavage of early to mid-Jurassic age (Sharp 1985, 1988). Units east of the Calaveras–Shoo Fly Fault contain two generations of subparallel structures of Paleozoic age (Merguerian 1982, 1985, Sharp 1985, Bhattacharyya 1986).

The Melones and Calaveras–Shoo Fly faults as well as the Bear Mountains fault zone, display multiple generations of subparallel structures. In many cases, we feel that these structures formed during a single period of non-coaxial deformation, and for reasons outlined elsewhere (Tobisch & Paterson 1988) treat them as a single 'composite' structure. Subscripts will be used to distinguish these composite structures, S_T, from continuous

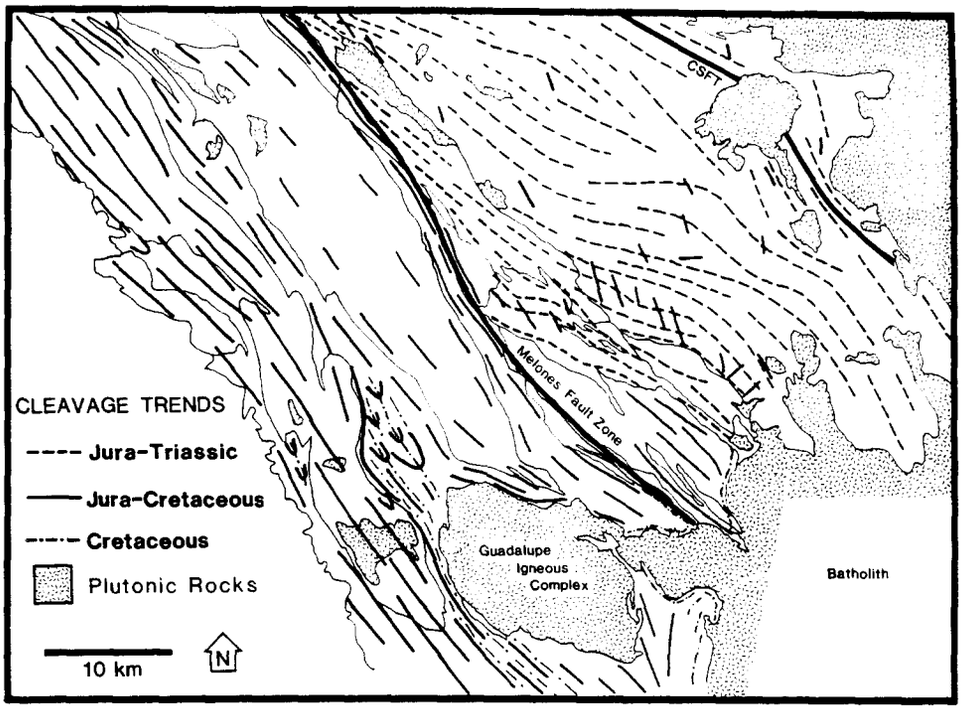

Fig. 3. Same area as Fig. 1 showing strikes (dips of cleavage are generally greater than 70°) of regionally developed cleavages (*Sc* or S_T) in southern portions of the Western Metamorphic Belt. The intensity of cleavage development is indicated by the relative spacing of cleavage strike lines. Previous work by Bateman *et al.* (unpublished work on the El Portal quadrangle), Mannion (1960), Best (1963), Bogen (1983) and Krauskopf (1985) has been incorporated into this figure. Paleozoic cleavages in the Northern Sierra terrane are subparallel to younger cleavages (Bhattacharyya 1986) and are not shown in this diagram.

cleavages, *Sc*, and crenulation cleavages, *Scc*, present in the Foothills terrane (*f*, for example Sc_f), Sullivan Creek and Merced River terranes (*m*), and Northern Sierra terrane (*n*).

Rock types and structures west of Melones Fault

Based on lithologic and structural features, the Foothills terrane can be divided into western, central and eastern zones (Fig. 1, Paterson *et al.* 1987a, Tobisch *et al.* in press). The western zone consists of a late Jurassic slate and greywacke sequence that overlies a sequence of volcanic breccias, tuffs, lavas and dikes or sills (Clark 1960, Tobisch *et al.* in press). The western zone is characterized by a sequence of late Jurassic interbedded slates and greywackes overlying Jurassic–Triassic volcanic rocks recently described by Bogen (1984). Separating the western and eastern zones is a central mélange zone consisting of metavolcanic and ultramafic blocks and lenses in a phyllite–metagreywacke matrix. Along the western margin of this central zone, lenses of serpentinite, talc schist and mylonitic volcanic rock mark the southern extension of the Bear Mountains fault zone (Paterson *et al.* 1987a).

One steep, NW-striking cleavage (Sc_f) occurs in the western zone and is axial planar to rare, open to isoclinal folds (Fc_f). Fold axes and extension lineations (Lc_f) plunge moderately to steeply to the southeast and are often but not always parallel. The metavolcanic rocks in the eastern zone generally lack cleavage except near contacts with slate/greywacke sequences and in some fine-grained units. Nearby slates and greywackes contain a variably developed cleavage which is axial planar to open to tight, gently plunging folds. Stretching lineations are rarely developed except for strong down-dip lineations near the Melones fault zone (Paterson & Wainger 1986).

The most commonly observed structures in the central Foothills belt are SE-plunging folds (Fcc_f) folding a well developed continuous cleavage or schistosity (Sc_f). Parallel or subparallel Lc_f and Lcc_f stretching lineations, defined by the alignment of minerals or rock fragments, and pressure shadows around porphyroblasts, plunge gently to steeply southeast with Lcc_f occasionally more strongly developed than Lc_f. The steep E-dipping Bear Mountains fault zone separates the central and western zones and was active from the late Jurassic to early Cretaceous. This fault has a largely reverse (east-over-west) sense but also some sinistral sense of motion (Paterson *et al.* 1987a). In this fault zone, different generations of structures are commonly transposed parallel to the shear zone forming a single composite structure S_T (Tobisch & Paterson 1988).

In summary, all three zones west of the Melones fault zone display a NW-striking cleavage and associated rare folds, but the intensity of development of these structures, outside of fault zones, decreases towards the east (Tobisch *et al.* 1987). *Lc* stretching lineations commonly plunge steeply to the southeast in the western zone, moderately to steeply southeast in the central zone, and are absent or only weakly developed in the eastern zone. *Fcc* folds and *Scc* cleavages are rare in the eastern zone,

locally developed in the western zone, and widespread in the central zone.

Rock types and structures between the Melones and Calaveras–Shoo Fly faults

The Sullivan Creek terrane is dominated by two large belts of metavolcanic rock separated by metasedimentary rocks composed of a matrix of phyllite and greywacke enclosing blocks of volcanic rock, pebbly mudstone, marble and chert. The eastern zone of metavolcanic rocks is early Jurassic (Bateman *et al.* 1985) whereas the western zone is late Jurassic (Clark 1964, Herzig 1985). Marble blocks in phyllite east of Bagby (B, Fig. 2) bear late Triassic and Mississippian fossils (A. Harris unpublished data 1986, Herzig 1985). A series of 169 Ma plutons intrudes these rocks (Herzig 1985, Sharp 1985) and thus the phyllite matrix must be older than 169 Ma and younger than the late Triassic marble blocks.

The metasedimentary rocks in the Sullivan Creek terrane gradually change to the east into a zone of argillite and some greywacke containing blocks and lenses of banded chert, pebbly mudstone and volcanic rock. The percentage of chert increases and that of greywacke decreases to the east (Bhattacharyya 1986). Blocks and bands of marble with Permian to early Triassic fossils are also present (Clark 1964, Bateman *et al.* 1985) These units form the Merced River terrane, but differ from Sullivan Creek units only in the greater proportion of chert and lesser amounts of volcanic rocks.

The older volcanic rocks in the Sullivan Creek terrane and metasedimentary rocks in both terranes contain a well-developed WNW–NW-striking continuous cleavage (Sc_m; Fig. 3) which is locally overprinted by a NW-striking domainal crenulation cleavage (Scc_m) and associated folds. The Sc_m cleavage is continuous across the Sullivan Creek–Merced River terrane boundary (Bhattacharyya & Paterson 1985). Stretching lineations, Lc_m, are commonly parallel to Fc_m axes and plunge steeply. In contrast, the belt of late Jurassic volcanic rocks in the Sullivan Creek terrane is only mildly deformed and does not commonly display folds or cleavages.

The Melones fault zone marks the western boundary of the Sullivan Creek terrane and represents an abrupt transition from Sullivan Creek structures and rock types to rock types and structures in the eastern Foothills terrane. This steep, E-dipping, ductile–brittle shear zone (Clark 1960, Paterson & Wainger 1986, and in preparation) is marked by a series of serpentinite lenses, intrusive rocks and lenticular slices of both hanging- and footwall rocks. The fault has a reverse (east-over-west) sense of motion. Structures are also complex, but essentially consist of a composite cleavage (Tobisch & Paterson 1988), formed during simultaneous fault motion and shortening of the western footwall, superimposed on older structures present in the Sullivan Creek terrane (Paterson & Wainger 1986).

Rock types and structures east of the Calaveras–Shoo Fly Fault

Rock types in this portion of the Northern Sierra terrane resemble those in the Merced River terrane except for the smaller percentage of chert and phyllite and a greater percentage of quartzite (Bhattacharyya 1986). Two sets of cleavages (Sc_n and Scc_n) which predate the continuous cleavage in the Merced River terrane are well developed in these rocks (Merguerien 1985, Bhattacharyya 1986). The dominant structure is Scc_n, which is defined by a crenulation cleavage or metamorphic banding: Sc_n is only preserved in microlithons of Scc_n. Near the Calaveras–Shoo Fly boundary these structures are deformed by open to close folds and associated crenulation cleavages.

Age of regional structures

West of the Melones Fault Sc_f must be late Jurassic or younger and previous workers have suggested an age of 155 ± 3 Ma (Schweickert *et al.* 1984). However, our recent work suggests a younger age (151–123 Ma) for Sc in the Foothills terrane and S_T in the Bear Mountains Fault (Paterson *et al.* 1987b, Tobisch *et al.* in press). East of the Melones Fault, work by Sharp (1983, 1985) indicates that Sc_m is approximately 177 Ma, although Schweickert *et al.* (1984) suggest that regional structures in the Sullivan Creek terrane are late Jurassic. In the Northern Sierra terrane, Sharp *et al.* (1982) and Sharp (1988) have reported radiometric ages from orthogneisses indicating two separate phases of magmatic activity at 370 ± 5 Ma, 275 ± 5 Ma, and when combined with structural studies suggest that the first cleavage is pre-370 Ma, whereas the second cleavage formed around 235 Ma (Merguerian 1985, Sharp *et al.* 1982, Sharp 1988).

Late phase or domainal structures

Late phase or locally developed structures occur throughout the region examined, but 70–90% of these structures occur in or near large ductile shear zones (Paterson in press). These include composite and late phase structures along the Bear Mountains, Melones and Calaveras–Shoo Fly faults, and in the ductile shear zones occurring along major lithologic boundaries. When domainal structures are considered separately from regional structures, it becomes apparent that multiple generations of regionally developed structures within a single terrane are not common in southern portions of the Western Metamorphic Belt. Outside of fault zones, we see one regionally developed cleavage in the Foothills terrane, a single but older cleavage in the Sullivan Creek and Merced River terranes, and two still older structures in the Northern Sierra terrane (Bhattacharyya 1986, Paterson 1986, Tobisch *et al.* 1987). The strains discussed below were obtained from samples not visibly affected by the deformation associated with the younger, domainal structures.

Regional metamorphism

Mineral assemblages in the area examined indicate that regional metamorphism mostly occurred under greenschist facies conditions. In the western Foothills terrane lower (chlorite) to upper (biotite) greenschist assemblages occur, whereas the central Foothills belt underwent a complex metamorphic history with conditions varying from lower greenschist to lower amphibolite grade (Tobisch *et al.* in press). Apparently these complexities increase to the south (Ehrreich 1965) and may, in part, be related to the emplacement of numerous dioritic intrusives and mafic to felsic dikes in this region. The degree of recrystallization decreases in the eastern Foothills terrane with quartz–sericite assemblages common in slates and greywackes and chlorite–epidote–albite ± prehnite(?) ± pumpellyite(?) assemblages occurring in metavolcanic rocks. The rare presence of detrital chlorite in slates and possible prehnite–pumpellyite assemblages in volcanic rocks suggest that metamorphic grade may locally decrease to prehnite–pumpellyite conditions in the eastern Foothills terrane (Behrman 1979, Sharp 1985, Day *et al.* 1986). East of the Melones Fault, units in the Sullivan Creek and Merced River terranes display assemblages indicative of lower greenschist facies metamorphism with color index data from conodonts indicating temperatures of 300–400°C (Bateman *et al.* 1985, A. Harris unpublished data 1986). In the study area, rock types in the Northern Sierra terrane show upper greenschist facies assemblages (Bhattacharyya 1986).

STRAIN ANALYSES

Introduction

We have measured total strains in 225 samples in various rock types including lapilli tuffs, volcanic breccias, pebbly mudstones, conglomerates, greywackes, slates and phyllites, and a small number of incremental strains using fibres in pressure shadows near pyrites, pyrite framboids and quartz grains. The samples analyzed are not evenly distributed, with a greater proportion located in the Sullivan Creek and Foothills terranes (Fig. 2). No quantitative data are available from the Northern Sierra terrane because at these latitudes this terrane lacks suitable markers.

The preparation of individual samples and measurement of strain are discussed elsewhere (Paterson in preparation) and are only summarized here. For clastic rocks, three perpendicular cuts have been made in oriented samples and the final ratio and orientation of objects measured. The techniques of Shimamoto & Ikeda (1976), Lisle (1977) and Miller & Oertel (1979) have been used to calculate two- and three-dimensional fabric ellipsoids. Corrections for the presence of primary fabrics were made by multiplying reciprocal 'primary fabric ellipsoids' calculated from non-deformed samples (Wheeler 1986, Paterson in preparation). When necessary Gay's (1976) equations have been used to correct for viscosity contrasts between clasts and matrix resulting in minimum estimates of whole rock strain for each sample (Paterson in preparation). Because of uncertainties in the corrections for primary fabrics, we have also calculated likely maximum strains and, where appropriate, quote both minimum and maximum values.

Strains in slates and phyllites were calculated using an X-ray, pole-figure goniometer under the supervision of Dr Gerhard Oertel (UCLA) following procedures outlined by Oertel (1970) and Tullis & Wood (1975). Incremental strains were determined from digitized fiber and rigid-object lengths following the procedures outlined by Beutner & Diegel (1985).

Relationship of strains to regional structures

Strain analyses provide three types of useful information: the orientation, intensity and type (constrictional, plane or flattening) of strain. Although the purpose of this paper is a regional synthesis of these types of data, it is useful first to examine the relationship between strains and nearby structures. If calculated strains are reliable, the following should hold true: (a) cleavage and strain intensities will show a systematic relationship; (b) the strain type will reflect the relative development of cleavages and stretching lineations; and (c) strain ellipsoid axes will show a close relationship to cleavage poles and lineations. We have found excellent agreement between the strains and the styles and orientations of regional cleavages and lineations at each sample locality with three exceptions. All three exceptions involved samples from ductile shear zones in regions where two or more cleavages are present. The close correspondence between regional structures and total strain suggests that the results from the measured strains can be extrapolated into regions where structural data are available using the techniques outlined by Schwerdtner *et al.* (1977).

Averaging strain data

Some means of averaging strain data is useful in attempting regional syntheses. One such method is to perform domainal analyses by separating strains by rock type, and then averaging strains over small domains. Oertel (1981) discusses methods for averaging strain data and we have used similar techniques in the present study. The domains selected are the western Foothills terrane, central Foothills terrane, domains near Moccasin, Virginia Mine and Bagby areas in the eastern Foothills and Sullivan Creek terranes, and domains in the Moccasin and Merced River areas in the Merced River terrane (Fig. 2). Within each domain, strain data are separated by rock type and structural setting (e.g. near intrusives, in fault zones). For each group arithmetic means of principal natural strains are calculated (thus ignoring the orientations of each ellipsoid, Oertel 1981) along with the ratios and orientation of the 'average directed ellipsoid' (thus taking the orientations of ellipsoids into account). The axial ratios obtained from these

two analyses are averaged in turn (Oertel 1981). The first calculation provides an arithmetic average of the shape and size of strain ellipsoids in a domain, but will tend to overestimate the bulk strain for that domain (Oertel 1981). The second method tends to underestimate bulk strain, and thus the additional averaging of the two sets of ratios is an attempt to better estimate the bulk strain. The arithmetically averaged strains for each domain are listed in Table 1 whereas the reaveraged directed strains for these domains are presented in Table 2. The above data represent averages of minimum values of strain because of the nature of corrections made for primary fabrics (Paterson in preparation). In Tables 1 and 2 the results have been calculated assuming that the long axis of the primary fabric ellipsoid is parallel to the long axis of the total strain ellipsoid. This may not always be the case, of course. It is, therefore, instructive to recalculate these averages using maximum values of strain calculated by assuming that the long axes of the primary fabric ellipsoids are at a high angle to the long axes of the measured fabric ellipsoids (Table 3). Actual strains probably lie between these two values but are likely to be closer to the minimum values listed in Table 2 because the maximum strains were calculated using geologically unlikely orientations for primary fabrics.

Intensities of strain

Intensities of total strain, E_s, are calculated from

$$E_s = 1/\sqrt{3}[(e_1 - e_2)^2 + (e_2 - e_3)^2 + (e_3 - e_1)^2]^{1/2}, \quad (1)$$

where e_1, e_2 and e_3 are principal natural strains (Hossack 1968). A comparison of Tables 2 and 3 indicates that although the intensities of total strains can be bracketed, exact values will remain uncertain until more is known about primary fabrics. However, these same figures suggest that the *relative* intensities of strains from one domain to the next can be determined with reasonable accuracy. In any one domain, the intensity of strain recorded will depend on the rock type. The lowest intensities are recorded by greywackes, and increasing intensities recorded in clast-supported conglomerates,

Table 1. Strain data calculated from arithmetic averages of principal natural strains for different rock types in each domain. The orientations of individual strain ellipsoids are not taken into account in these calculations. In each domain, samples are listed in order of increasing strain intensity. The same domains, lithologic groups and sample sizes were used in calculating data for Tables 2 and 3

Rock type	Number of samples	Per cent extension X	Y	Z	Strain intensity	Lode's parameter
Western Foothills terrane:						
Lapilli tuff	21	99	5	−52	1.02	0.11
Pebbly mudstone	6	104	21	−59	1.17	0.35
Slate	2	273	34	−80	2.10	0.30
Central Foothills terrane:						
Greywacke	7	72	−6	−38	0.73	−0.17
Lapilli tuff	5	68	−2	−39	0.72	−0.07
Pebbly mudstone	4	92	8	−52	0.99	0.18
Eastern Foothills terrane:						
Bagby:						
Greywacke	7	17	5	−19	0.27	0.43
Lapilli tuff	8	23	8	−25	0.36	0.46
Slate	6	75	33	−57	1.05	0.61
Virginia Mine:						
Conglomerate	4	40	14	−37	0.59	0.49
Greywacke	4	56	7	−40	0.68	0.20
Moccasin:						
Greywacke	6	8	3	−10	0.14	0.50
Conglomerate	4	40	11	−35	0.56	0.39
Slate	4	50	29	−48	0.82	0.73
Sullivan Creek terrane:						
Bagby:						
Pebbly mudstone	9	135	−5	−55	1.17	−0.10
Briceburg:						
Lapilli tuff	7	96	5	−51	0.99	0.10
Virginia Mine:						
Lapilli tuff	3	98	13	−55	1.06	−0.25
Pebbly mudstone	6	108	9	−56	1.10	0.17
Moccasin:						
Lapilli tuff	13	177	3	−64	1.45	0.05
Merced River terrane:						
Briceburg:						
Pebbly mudstone	10	96	−8	−45	0.90	−0.19
Slate	7	89	41	−62	1.21	0.63
Moccasin:						
Pebbly mudstone	17	168	4	−67	1.42	0.06
Slate	9	124	46	−69	1.48	0.57

lapilli tuffs, pebbly mudstones and slates (Tables 2 and 3). A more detailed look at the degree of this lithologic control is obtained by examining strains in adjacent samples but from different rock types (Table 4). Differences in strain intensity are most spectacular in slate and greywacke sequences where slates commonly record strain intensities 3–4 times those in greywackes (however, see section on volume reductions). Smaller differences in intensity and large differences in strain type also occur in individual samples across contacts between metavolcanic and metasedimentary rocks. Similar differences are seen in the arithmetic and directed averages calculated for different rock types in each domain (Tables 1–3).

Regional variations in strain intensity are best examined by comparing data from similar rock types. In all rock types, strain intensities are moderate to high in the western Foothills terrane, decrease in value in the central Foothills and reach the lowest values in the eastern Foothills terrane (Table 2). East of the Melones Fault, strain intensities immediately increase to values similar to, or greater than, those observed in the western Foothills, and generally maintain these high values throughout the Sullivan Creek and Merced River terranes. Variations also occur within each domain, although to a lesser degree than the variations between domains. For example, in the eastern Foothills terrane, strain intensities reach their lowest values in the Moccasin area, whereas in the Sullivan Creek and Merced River terranes strains reach their highest values in this same region (Tables 2 and 3).

Orientation of strain ellipsoids

The strike/dip of the XY plane and plunge/trend of the X axis ($X > Y > Z$) of measured strain ellipsoids are plotted on equal-area projections (Fig. 4) and average orientations determined. The averages for each domain are listed in Table 5 along with the orientations of the mean directed ellipsoids calculated from different rock types in each domain. Although some scatter in the orientations of XY planes is present in every domain, regional patterns are certainly recognizable. In most cases dips are steep, usually ranging between 70 and 90°.

Table 2. Strain data calculated from the average matrix nôtation (directed strains of Oertel 1981) for the lithologic groups in each domain. Because the matrix form of individual strain ellipsoids takes into account the orientation of the ellipsoid, average orientation data can be determined from the final matrix. Note that strain intensities are always lower than those in Table 1, but that no consistent change in strain type is recognizable

Rock type	Per cent extension			Orientation		Strain intensity	Lode's parameter
	X	Y	Z	X	XY		
Western Foothills terrane:							
Lapilli tuff	84	6	−49	87/107	332/88	0.91	0.14
Pebbly mudstone	87	26	−58	85/147	142/89	1.09	0.47
Slate	187	48	−76	75/158	148/87	1.83	0.47
Central Foothills terrane:							
Greywacke	46	−4	−29	68/78	53/80	0.51	−0.17
Lapilli tuff	40	1	−29	5/351	349/66	0.48	0.03
Pebby mudstone	86	10	−51	78/130	355/82	0.95	0.22
Eastern Foothills terrane:							
Bagby:							
Greywacke	14	6	−18	67/23	320/69	0.25	0.56
Lapilli tuff	20	4	−20	24/143	339/58	0.29	0.28
Slate	68	29	−54	45/116	319/69	0.97	0.60
Virginia Mine:							
Conglomerate	36	16	−38	54/145	329/87	0.57	0.59
Greywacke	52	8	−39	60/335	326/84	0.66	0.25
Moccasin:							
Greywacke	6	2	−8	56/311	145/81	0.11	0.49
Conglomerate	26	7	−25	10/299	122/73	0.38	0.38
Slate	39	26	−43	48/301	126/85	0.68	0.78
Sullivan Creek terrane:							
Bagby:							
Pebbly mudstone	129	−5	−54	84/6	307/85	1.14	−0.09
Briceburg:							
Lapilli tuff	91	2	−49	82/11	317/83	0.93	0.05
Virginia Mine:							
Lapilli tuff	85	15	−53	79/89	310/83	0.98	0.30
Pebbly mudstone	99	11	−55	65/19	315/67	1.05	0.21
Moccasin:							
Lapilli tuff	139	10	−62	69/334	293/76	1.30	0.15
Merced River terrane:							
Briceburg:							
Pebbly mudstone	75	−11	−35	68/176	3/87	0.72	−0.36
Slate	81	43	−61	75/299	293/89	1.18	0.70
Moccasin:							
Pebbly mudstone	134	11	−61	69/336	294/75	1.28	0.17
Slate	118	38	−67	81/318	290/86	1.39	0.51

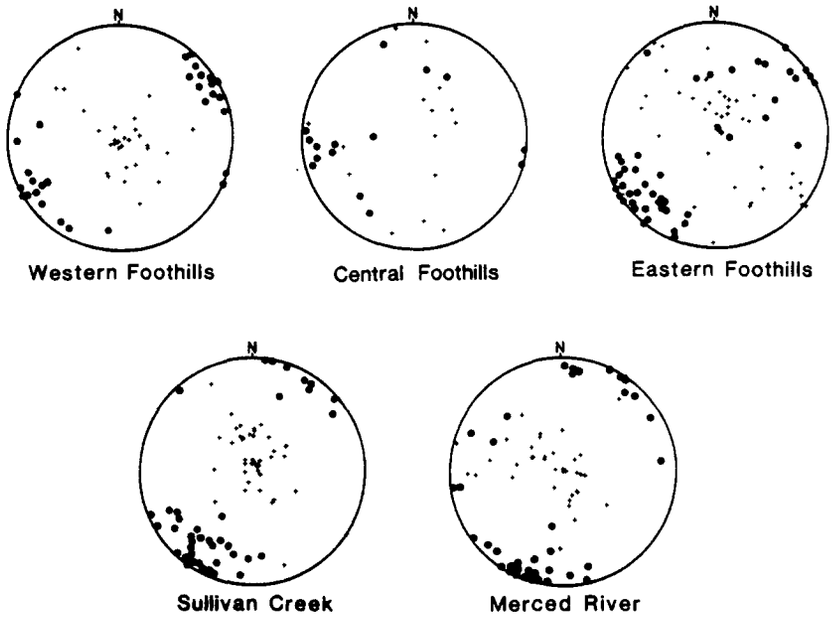

Fig. 4. Equal-area projections of the orientations of XY planes and X axes of strain ($X > Y > Z$) associated with regionally developed cleavages from different domains. Circles represent poles to the XY planes; the crosses represent X axes.

Table 3. Average directed ellipsoid data calculated as in Table 2, but using maximum corrected strain data (i.e. X axes of primary fabric ellipsoids oriented perpendicular to bedding; see text for actual procedures used). Primary fabric corrections for slates were treated differently than other rock types (see text, or Paterson in preparation). Thus, for the sake of comparison, data from slates listed in Table 2 are reproduced here

Rock type	Per cent extension X	Y	Z	Orientation X	XY	Strain intensity	Lode's parameter
Western Foothills terrane:							
Lapilli tuff	114	7	−56	87/112	333/88	1.12	0.12
Pebbly mudstone	125	28	−65	82/145	142/90	1.37	0.40
Slate	221	25	−72	15/329	152/81	1.75	0.23
Central Foothills terrane:							
Greywacke	62	1	−39	40/222	50/80	0.70	0.03
Lapilli tuff	57	2	−37	5/350	348/69	0.65	0.07
Pebbly mudstone	168	12	−67	59/153	345/83	1.48	0.16
Eastern Foothills terrane:							
Bagby:							
Greywacke	22	9	−27	69/17	319/72	0.41	0.49
Lapilli tuff	96	51	−66	38/13	346/60	1.34	0.71
Slate	67	26	−52	28/126	317/70	0.92	0.55
Virginia Mine:							
Conglomerate	67	14	−47	86/48	318/86	0.83	0.34
Greywacke	69	10	−46	58/335	324/83	0.82	0.26
Moccasin:							
Greywacke	14	6	−17	32/316	146/75	0.24	0.55
Slate	40	23	−41	36/303	127/85	0.67	0.70
Conglomerate	39	10	−34	67/56	303/67	0.54	0.37
Sullivan Creek terrane:							
Bagby:							
Pebbly mudstone	168	6	−65	76/22	313/77	1.43	0.08
Briceburg:							
Lapilli tuff	138	7	−61	79/18	329/81	1.28	0.12
Virginia Mine:							
Lapilli tuff	116	16	−60	79/87	310/83	1.21	0.26
Pebbly mudstone	143	12	−63	64/18	315/67	1.35	0.18
Moccasin:							
Lapilli tuff	185	16	−70	69/335	294/76	1.59	0.20
Merced River terrane:							
Briceburg:							
Pebbly mudstone	96	−10	−43	63/175	0/87	0.89	−0.26
Slate	78	43	−60	88/64	294/88	1.15	0.71
Moccasin:							
Pebbly mudstone	174	10	−67	84/359	284/84	1.50	0.14
Slate	139	35	−69	85/66	284/87	1.44	0.27

Table 4. Comparison of strain data from lithologically different but adjacent samples. All samples have been corrected for the presence of primary fabrics but not corrected for possible volume losses. Note the change in both intensity and type of strain across lithologic contacts

Sample	Rock type	Distance apart	Per cent extension X	Y	Z	Strain intensity	Lode's parameter
Ba-4	Greywacke	20 cm	18	7	−21	0.30	0.51
Ba-5	Slate	—	80	31	−58	1.08	0.56
Br-27	Slate	15 m	90	64	67	1.38	0.85
EP-37	Lapilli tuff	—	55	3	−37	0.64	0.11
Br-65	Lapilli tuff	40 m	195	0	−66	1.53	0.00
Br-66	Pebbly mudstone	—	126	71	−74	1.67	0.74
Mo-67B	Phyllite	20 m	99	31	−62	1.21	0.49
Mo-68	Lapilli tuff	—	145	1	−60	1.28	0.02
Mo-76A	Slate	2 m	45	27	−48	0.76	0.74
Mo-76B	Greywacke	—	12	8	−17	0.23	0.76
Mo-76C	Gritty greywacke	—	12	4	−14	0.19	0.41
Mo-108	Conglomerate	50 m	12	4	−14	0.20	0.42
Mo-109B	Slate	—	50	38	−51	0.89	0.85
Mo-109C	Greywacke	20 m	9	1	−10	0.14	0.21
Mo/110A	Slate	50 cm	47	24	−45	0.75	0.66
Mo-110B	Greywacke	—	13	10	20	0.28	0.85
IG-22A	Greywacke	50 cm	146	−28	−43	1.11	−0.69
IG-22B	Slate	—	161	19	−68	1.49	0.25

The only common exceptions are in samples from F_2 folds in the central Foothills terrane, and in some of the more weakly deformed samples in the eastern Foothills terrane. All domains west of the Melones fault zone display XY planes striking in more northerly directions in contrast to WNW strikes in domains east of the fault. A closer examination of these data suggests that strikes of XY planes are gradually changing across the Western Metamorphic Belt from 293° in the Merced River terrane to 303° in the Sullivan Creek terrane, 320° in the eastern Foothills terrane, to 331° in the western Foothills terrane, although a sharp break in the orientation and age of strains does occur across the Melones fault zone (Paterson & Wainger 1986). The central Foothills terrane displays somewhat anomalous northerly orientations (Table 5) that reflect the transposition to more northerly strikes of a NW-striking Sc_f by Fcc_f during movement along the Bear Mountains Fault (Paterson *et al.* 1987).

In every domain X axes of the strain ellipsoids show some scatter along planes parallel to regional cleavages (Fig. 4). Some of this scatter may be anomalous because small errors in analyses of samples with low strains (e.g. greywackes in the Moccasin area) or of samples with

Table 5. Summary of the orientations of X axes and XY planes of total strain ellipsoids. Averages for each domain were determined from statistical analyses of data plotted in Fig. 4. Directed strain ellipsoid averages from various rock types were calculated from minimum strain data (Table 2) using procedures discussed by Oertel (1981). Orientation data from the central Foothills zone (CFZ) are unreliable due to large-scale refolding

Area	Average from individual samples XY plane	X axis	Rock type	Directed ellipsoid averages XY plane	X axis
WFT	331/87	85/142	Lapilli tuff	333/85	84/104
			Pebbly mudstone	138/88	75/145
			Slate	152/81	15/329
CFT	351/74	66/31	Lapilli tuff	352/70	7/169
			Pebbly mudstone	353/82	81/118
			Greywacke	46/73	67/91
EFT	320/83	70/357	Lapilli tuff	342/58	26/144
			Pebbly mudstone	301/79	79/22
			Slate	317/70	28/126
			Greywacke	320/69	64/14
			Conglomerate	140/85	34/143
SCT	303/79	78/357	Lapilli tuff	320/84	82/10
			Pebbly mudstone	307/84	82/10
MRT	293/87	84/186	Briceburg:		
			Pebbly mudstone	171/89	69/174
			Slate	294/88	88/64
			Moccasin:		
			Pebbly Mudstone	293/79	56/310
			Slate	284/87	85/66

large flattening strains (e.g. slates throughout the Foothills terrane) may result in large errors in X axis orientations. Regardless, X axes tend to be steep in the western Foothills terrane, in the Bear Mountains and Melones fault zones, and in the Sullivan Creek and Merced River terranes. Gently plunging X axes are more common in the central and eastern Foothills terranes, particularly in weakly strained samples outside fault zones.

Strain types

Strain types (Hossack 1968) are calculated from equation (2)

$$\nu = [2(e_2) - e_1 - e_3]/[e_1 - e_3], \quad (2)$$

where ν is the Lode's parameter. Prior to examining strain types (defined as prolate, plane or oblate), two factors that influence these values need to be mentioned. Small errors in samples with low strains can cause large errors in the calculated shape of the strain ellipsoid. Thus, some caution is needed when interpreting strain types from the weakly strained samples in the eastern Foothills terrane. Also, the scatter of X axes in cleavage planes will tend to increase Lode's parameters (move strain types towards the flattening axis on a Hsu or Flinn plot) when these samples are used to calculate average directed ellipsoids. If the scatter of X axes is due to the errors in orientations noted above, then misleading ellipsoid shapes may be obtained. Nevertheless, strain types are more a function of rock type than location (Tables 2 and 3). Greywackes and phyllosilicate-rich rocks tend to develop flattening strains, and lapilli tuffs approach plane strain. Conglomerates tend to record a range of strain types, although in matrix-supported conglomerates Lode's parameters increase with an increasing percentage of phyllosilicates. Several interesting exceptions occur. First, more constrictional strain types are common in some rock types from the central Foothills terrane, particularly near the Bear Mountains fault zone. The multiple generations of folds and lineations in this area indicate that the measured ellipsoids reflect the superposition of more than one period of folding. In hinges of *Fcc* folds, X axes of pre- and syn-folding strain ellipsoids are parallel but the Z axes are perpendicular, resulting in constrictional-type total strains (e.g. Kligfield *et al.* 1981a,b). However, these constrictional strains also occur outside of *Fcc* hinges. Beyond suggesting that these constrictional strains reflect complex deformation along the Bear Mountains Fault, their cause is uncertain.

Another exception is the mildly constrictional strains recorded by pebbly mudstones in the Merced River terrane east of Briceburg (Br in Fig. 2). Bhattacharyya (1986) has suggested that the constrictional strains in the Merced River terrane may represent a region of 'return flow' needed to compensate for the flattening strains observed nearby. Alternatively, Freeman (1987) noted that constrictional strain types may develop due to large viscosity contrasts existing between clasts and matrix.

Magnitude and effect of volume losses on strains

The fact that large flattening ellipsoids commonly occur in most slates, greywackes and some pebbly mudstones (Table 2) raises the question of how much the contrast in strain type and intensity between different rock types can be explained by bedding-parallel compactions or deviatoric volume losses. Bulk strains in the volcanic rocks indicate that these belts record plane strain. Our observations suggest that it is unlikely that the volcanic rocks underwent significant volume changes, and suggest that the strain data obtained from these belts are largely the result of tectonic deformation. If the same assumption is made for the slate/greywacke sequences lying between these volcanic belts, we are faced with the problem of explaining why large extensions occur parallel to the orogen in slate/greywacke sequences while the surrounding metavolcanic rocks underwent plane strain. We are faced with the same problem on a centimeter-scale when examining the slate/greywacke sequences. Large bedding-parallel extensions would have to occur in the slates while centimeters away the greywackes are only mildly deformed. An attractive alternative is that the slates, greywackes and some pebbly mudstones underwent different amounts of deviatoric volume loss, and that all units subsequently underwent a tectonic strain of plane type.

In order to examine this possibility, we have algebraically decomposed final oblate ellipsoids into plane strain and pure flattening ellipsoids (Fig. 5). In samples where bedding and cleavage are parallel, the plane strain ellipsoid represents the minimum amount of tectonic strain that must have occurred in the sample, whereas the pure flattening ellipsoid represents the largest amount of bedding-parallel compaction possible for that sample.

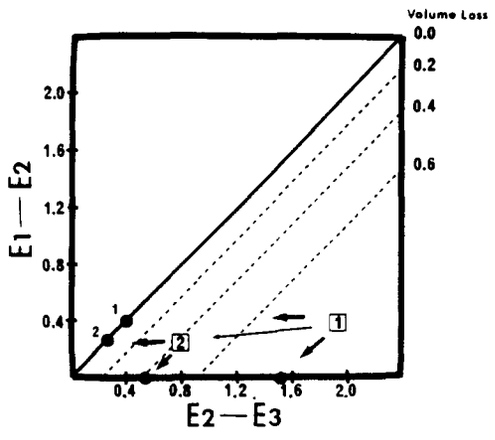

Fig. 5. Log deformation or modified Flinn plot displaying the decomposition of any final strain in the flattening field into a plane strain and a pure flattening strain (strain 1 going to dots labelled 1). The pure flattening strain is the maximum amount of compaction or deviatoric volume loss possible in the sample, whereas the plane strain is the minimum amount of tectonic strain (see text). Where adjacent volcanic and slate samples are available, the strain recorded in the volcanic rock is first removed from the slate (strain 1 to strain 2) and the resulting strain then decomposed (strain 2 going to dots labelled 2). Decomposition in both cases is done algebraically. The distances between the pure flattening strains bracket the amount of volume loss for the slate (see text).

Table 6. Possible deviatoric volume losses and subsequent tectonic strains in adjacent samples. Volume losses given in terms of per cent shortening along Z, whereas strains are presented in terms of extensions along the X, Y and Z axes. Volume losses and subsequent strains were calculated as discussed in text

Sample	Rock type	Volume loss		Tectonic strain					
				Minimum			Maximum		
		Minimum	Maximum	X	Y	Z	X	Y	Z
EP-37	Lapilli tuff	0.00	−0.09	49.80	0	−33.29	54.63	3.30	−37.40
Br-27	Slate	−0.43	−0.78	13.92	0	−22.40	54.44	35.85	−52.33
Mo-68	Lapilli tuff	0.00	−0.03	142.66	0	−58.79	145.10	1.02	−59.61
Mo-67B	Slate	0.00	−0.57	52.55	0	−34.45	99.17	30.58	−61.55
Br-65	Lapilli tuff	0.00	0.00		—		195.38	−0.31	−66.04
Br-66	Pebbly mudstone	0.00	−0.80	32.54	0	−24.55	126.09	70.59	−74.07
Ba-4	Greywacke	0.00	−0.18	10.5	0	−9.50	18.26	7.02	−20.99
Ba-5	Slate	−0.55	−0.58	37.49	0	−27.27	38.42	0.21	−27.91
Mo-110B	Greywacke	0.00	−0.26	2.64	0	−2.57	13.35	10.44	−20.12
Mo-110A	Slate	−0.47	−0.50	18.57	0	−15.66	18.89	0.47	−16.28
Mo-76B	Greywacke	0.00	−0.20	3.64	0	−3.52	11.65	7.72	−16.86
Mo-76C	Coarse greywacke	0.00	−0.10	7.94	0	−7.35	11.82	3.59	−13.67
Mo-76A	Slate	−0.52	−0.54	13.77	0	−12.10	13.44	0.25	−12.06
Mo-109C	Greywacke	0.00	−0.04	7.83	0	−7.26	9.26	1.33	−9.67
Mo-109B	Slate	−0.61	−0.63	8.97	0	−8.23	9.21	0.02	8.46
Mo-108	Conglomerate	−0.10	−0.11	7.60	0	−7.24	12.25	3.79	−14.16

Such bedding-parallel compactions can form due to extension in bedding and shortening perpendicular to bedding, or by deviatoric volume changes causing compaction along Z and *no* extension in the bedding plane (Engelder & Oertel 1985). The common parallelism between bedding and cleavage in the Western Metamorphic Belt allows us to calculate maximum possible volume reductions, along with the resulting minimum tectonic strains in the above fashion for individual samples (Table 6) and domains (Table 7).

Some information about minimum values of volume loss in slaty rocks can also be obtained using the following procedure. For slates adjacent to lapilli tuffs, we assume that the slates underwent at least as much tectonic strain as the volcanic rocks and remove (multiply by reciprocal ellipsoid) this strain from the slate. If the resulting ellipsoid has an oblate shape, it can be decomposed into plane strain and pure flattening ellipsoids (Sanderson 1976). The pure flattening ellipsoid is used to calculate volume reductions as discussed previously.

Table 7. Summary of deviatoric volume losses and subsequent tectonic strains estimated from average directed minimum strains in each domain (Table 2). The volume loss calculations are discussed in the text. Note that when maximum volume loss estimates are used to calculate subsequent minimum tectonic strains, the strain in slates may drop below that of nearby lapilli tuffs. This does not seem likely to us and suggests that minimum volume loss estimates (when available) better represent volume losses

Area	Rock type	Volume loss		Tectonic strain					
				Minimum % extension			Maximum % extension		
		Minimum	Maximum	X	Y	X	X	Y	Z
WFT	Lapilli tuffs	0.00	−0.11	92	0	−48	104	6	−51
	Pebbly mudstones	−0.07	−0.38	74	0	−43	100	15	−56
	Slates	−0.49	−0.55	189	0	−65	200	4	−68
EFT	Bagby:								
	Lapilli tuffs	0.00	−0.03	19	0	−16	25	9	23
	Greywackes	0.00	−0.14	12	0	−10	18	6	−19
	Conglomerates	0.00	−0.21	28	0	−22	29	1	−24
	Slates	−0.56	−0.57	32	0	−24	34	1	−26
EFT	Moccasin:								
	Greywackes	0.00	−0.09	5	0	−4	8	3	−10
	Slates	−0.48	−0.54	16	0	−14	19	3	−18
Sullivan Creek and Merced River terranes									
	Briceburg:								
	Lapilli tuffs	0.00	−0.11	89	0	−47	104	8	−49
	Pebbly mudstones	0.00	0.00		—		108	−5	−44
	Slates	−0.34	−0.64	34	0	−25	57	24	−48
	Moccasin:								
	Lapilli tuffs	0.00	−0.04	164	0	−63	187	9	−60
	Pebbly mudstones	0.00	−0.06	154	0	−61	180	9	−60
	Slates	−0.27	−0.57	74	0	−43	111	19	−60

The plane strain ellipsoid represents the additional tectonic strain in the slate not recorded by the volcanic sample.

A slightly different procedure is used in adjacent slate/greywacke or greywacke/conglomerate samples. The final ellipsoid in the greywacke is decomposed into plane strain and pure flattening ellipsoids and possible volume reductions in greywackes calculated from the flattening ellipsoid. The plane strain in the greywacke is then removed from the slate and the resulting ellipsoid dealt with as in the previous example. Using the maximum values of volume losses and subsequent minimum strains calculated above, limits can be placed on volume losses and tectonic strains (Table 7). For slates these volume loss estimates range from −43% to −78% in individual samples and from −27% to −64% in domains. In the Foothills terrane, the estimated brackets are much tighter, suggesting volume losses between −48% and −55%. Such volume losses in slates are compatible with volume losses noted elsewhere (Wright & Platt 1982, Boulter 1986, Ellis 1986, Davison 1987). Estimated volume losses in greywackes, conglomerates and most pebbly mudstones tend to be much lower, ranging from 0% to −26% (see also Davison 1987).

A check of the assumption that bulk strains in volcanic rocks are of plane type can be made by algebraically decomposing final strain ellipsoids in volcanic rocks into plane strain and compaction ellipsoids. Although values of volume loss in individual samples range up to −11%, they are commonly near 0% corroborating our initial assumption of little to no volume loss in these rocks.

Other combinations of volume loss and tectonic strain are certainly compatible with the total strains obtained in this study. However, if larger volume losses for slates are assumed, then tectonic strains in slaty rocks must be much lower than strains in nearby volcanic rocks. If lower volume losses are assumed then the problem of large extensions parallel to the orogen must be dealt with both on a regional scale and in the slate/greywacke sequences. Given our present understanding of the structures in each region and the mechanical behaviour of different rock types, we find either of these suggestions unlikely. In the following discussion, we assume that slates have undergone volume losses of −45% to −65%, greywackes and pebbly mudstones volume losses of 0% to −26%, and volcanic rocks less than −10% volume loss, unless otherwise noted.

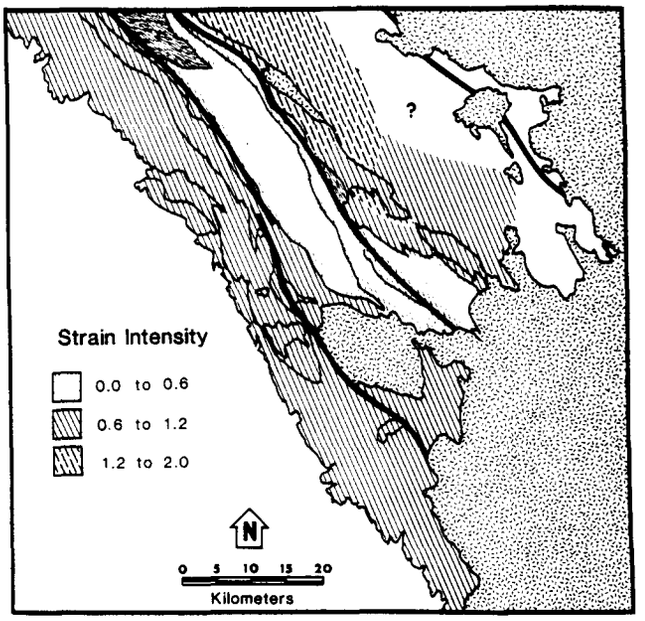

Fig. 6. Strain intensity map displaying zones with similar values of tectonic strain. Note that the Bear Mountains and Melones fault zones represent significant strain discontinuities with two exceptions. Late Jurassic volcanic rocks ,east of (or in?) the Melones Fault record anomalously low values, and regions in the central Foothills belt near the Guadalupe Igneous Complex (GIC) record anomalously high values. See text for discussion.

Regional patterns of tectonic strain

The values of whole rock strains and volume loss estimates allow us to construct maps displaying the average intensity of tectonic strains. To do so, strains due to compaction are first removed from appropriate samples. We then plot values of tectonic strain intensity and attempt to recognize regions of similar values of strain. In doing so, we have used the close correspondence between measured strains and observed structures noted earlier, along with the procedures of Schwerdtner *et al.* (1977) to extrapolate strain data into areas where only structural data are available.

Three regions displaying distinct strain intensities are clearly discernible (Fig. 6). West of the Bear Mountains Fault, strain intensities are moderate to high, ranging from 0.6 to 1.5., whereas between the Bear Mountains and Melones faults intensities fall below 0.6 and are commonly less than 0.3. East of the Melones Fault intensities are moderate to high and fall between 1.0 and 2.0. Strain intensities range up to 2.9 in the Melones fault zone (Paterson & Redfield 1984, Paterson & Wainger 1986) and in a few scattered samples from the Bear Mountains Fault (Tobisch *et al.* 1987). Two exceptions to this pattern occur: the upper Jurassic volcanic rocks immediately east of the Melones Fault record anomalously low strains, and southern portions of the central Foothills terrane display somewhat high values. Reasons for these anomalies will be discussed later.

Strains in fault zones

Patterns of strain in the Bear Mountains and Melones fault zones have been examined by Paterson & Redfield (1984), Paterson & Wainger (1986, and in preparation) and Paterson *et al.* (1987a). Strain intensities in both of these zones are heterogeneous ranging from small in resistant blocks to some of the largest intensities measured in the study area. Strain types are usually

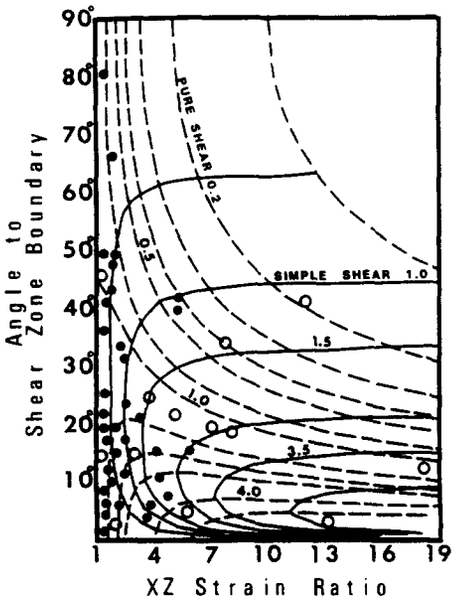

Fig. 7. X/Z ratios of strain plotted against the orientation of the X axis of total strain on curves displaying various amounts of simple or pure shear (after Coward & Kim 1981 and Kligfield *et al.* 1981a). Data from the Melones fault zone. Note that data from within the fault (open circles) suggest that increasing amounts of simple shear are needed to get final ratios and orientations. Comparison of this data with plots in Kligfield *et al.* (1981a) indicate that no additional volume loss is occurring during deformation within the fault zone.

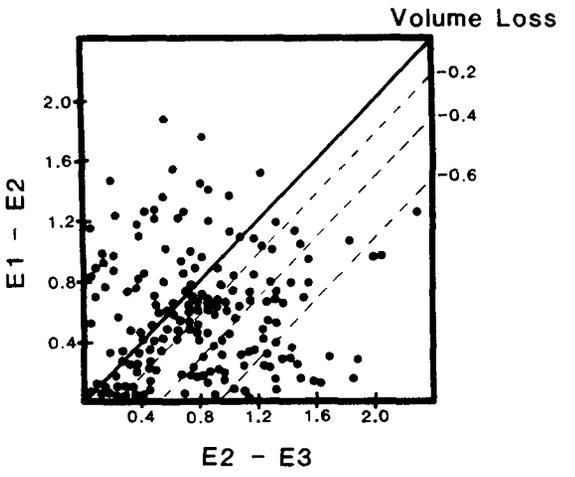

Fig. 8. Log deformation or modified Flinn plot of strain data from the Western Metamorphic Belt.

plane to flattening. Both the Melones and Bear Mountains fault zones mark boundaries across which values of strain intensity associated with regional cleavages change significantly (Fig. 6).

An attempt was made to determine if the strains in these fault zones are the result of simple shear, simple shear plus volume loss, or simple plus pure shear using the techniques outlined by Coward & Kim (1981) and Kligfield *et al.* (1981). Data from slates, pebbly mudstones and greywackes have been corrected for volume loss due to early compactions. Thus, volume losses in this analysis are additional losses incurred during fault motion. Strains from within the fault zones along with wallrock strains were plotted on graphs displaying curves representing various combinations of simple shear, pure shear or volume loss (available constraints do not allow examining combinations of all three, e.g. Kligfield *et al.* 1981a). Wallrock strains are most compatible with a combination of pure shear plus a small component of simple shear, whereas strains in the fault zones require an increasingly large component of simple shear (Fig. 7). The strain data from the Foothills terrane are therefore most compatible with the hypothesis that the large domains between the faults underwent largely pure shear and that these domains are separated by ductile shear zones that underwent pure plus simple shear. This suggestion is supported by a variety of structures (Tobisch *et al.* in press), particularly the common presence of curved fibers in strain shadows and other shear sense indicators in the fault zones and largely straight fibers and absence of shear indicators in the wallrocks.

DISCUSSION

Heterogeneous nature of strain

If the data from all 225 samples are plotted on one Flinn diagram (Fig. 8), a rather impressive scatter results, clearly indicating that strain patterns in this region are complex. Some order can be made out of this scatter by grouping strains by rock type, structural setting and geographic distribution. Although samples have been analysed from all of these settings, the average values of strain discussed in this paper have been calculated from such groups most representative of the regional structures (Sc or Scc_m) and, in general, do not reflect the heterogeneity of strains found in ductile shear zones or near intrusives. Some of the heterogeneity in strain may be due to small errors in analyses. However, we suggest that most of the heterogeneity in strain is due to lithologically-controlled strain partitioning (Ramsay 1982, Bell *et al.* 1986). It is important to remember, however, that *the heterogeneity in total strains does not just reflect partitioning of tectonic strains, but also reflects small differences in primary fabrics and large differences in volume losses recorded by different rock types.*

Volume loss estimates

If the volume loss estimates calculated above are correct, these results suggest several interesting conclusions, the first of which is that contrasts in strain intensities still exist between different rock types but are much lower than the original estimates (compare tectonic strains in Tables 2 and 6). After removal of strains due to deviatoric volume losses, the largest difference in tectonic strain in different rock types is now less than 2 to 1 and in many cases much smaller. The second observation is that volume losses appear to be more uniform throughout the region examined (in similar rock types) than tectonic strains. For example, strains are quite low

in the eastern Foothills terrane, but calculated volume losses in this region are high. This suggests that volume losses are not strictly dependent on the intensities of strain or age of units.

A third point of interest is that even after volume reductions of 45–65%, many of the slates still record small flattening strains. This indicates that although plane strain may occur on a regional scale, small amounts of orogen-parallel extension develop in small domains. The scatter in orientation of X axes for calculated strain ellipsoids in other rock types (Fig. 4) and low plunges of averaged ellipsoids in some domains (Table 2) indicate that such extensions are present in other rock types as well. These extensions when projected into a horizontal plane range from 1% to 20% and may be compensated for by constrictional strains recorded in individual samples (Fig. 5) or in larger domains of vertically-oriented constrictional flow (pebbly mudstones in the Merced River terrane).

Strain discontinuities along faults and lithologic contacts

Both averaged strain data from large domains (Table 2) and comparisons of strains in individual samples (Table 4) indicate that lithologic contacts and large fault zones represent discontinuities in total strain. Even after taking into account the effect of variations in primary fabric and volume losses, discontinuities in tectonic strain exist across the contacts and faults. Do these differences in tectonic strain indicate that the lithologic contacts, as do the fault zones, represent displacement discontinuities? The lithologic contacts vary in scale from major contacts between metavolcanic belts and surrounding metasediments to contacts between interbedded slates and greywackes. The large metavolcanic–metasedimentary contacts resemble ductile shear zones in the following ways: (a) cleavage and strain intensities in both rock types increase near these zones (compare sample pairs in Table 4 to domain averages in Table 2); (b) strain types are variable but commonly more oblate; (c) units are disrupted and intermixed along the zones; and (d) younger, domainal structures are commonly present. These features can be explained if the volcanic belts are acting as large viscous blocks surrounded by a matrix of less viscous slates. For example, if the overall shortening in a region is 50%, but volcanic belts in that region only shorten 40%, the 'excess' strain not taken up by the volcanic rocks will concentrate along the boundaries of these belts. The difference in strain in the two rock types can be accommodated by slip along a décollement at the contact or by the development of a ductile shear zone. The large flattening strains along the contacts may reflect the strain type needed in order to maintain a continuum as the slates/greywackes flow around the volcanic blocks. A similar apportioning of strain also occurs near plutons (Castro 1986) and porphyroblasts (Bell *et al.* 1986).

The smaller size of the slate/greywacke contacts makes it difficult to determine the characteristics of these discontinuities; however, the differences in strain intensity and type, along with the differences in volume estimates from adjacent slate and greywacke samples indicate that these contacts do represent strain discontinuities. In slate/greywacke sequences in the Bagby area (B in Fig. 2), striations observed only on bedding surfaces and oriented at an angle to stretching lineations, suggest that some slip has occurred along bedding surfaces. In thin section, concentrations of opaque material along these contacts indicate that material was preferentially removed along the contacts. But whether or not each contact represents a sharp discontinuity along which slip has occurred, or if strains gradually change near these contacts is unclear.

The Bear Mountains, Melones and Calaveras–Shoo Fly faults are distinct from the large-scale lithologic contacts in three ways: (1) structural/strain histories are distinct from one side of the fault to the other; (2) exotic rock types are often found in these zones; and (3) faults do not always occur along lithologic boundaries. Thus, a distinction should be made between regionally developed shear zones, which are likely candidates for terrane boundaries, and shear zones along lithologic boundaries, which may reflect only the discontinuity in strain between two rock types.

For two of the faults, the Melones and Calaveras–Shoo Fly, the extent to which younger deformations on one side of the fault overprint older deformations on the other side is crucial to our understanding of the genesis of terranes in the Western Metamorphic Belt. Along the Calaveras–Shoo Fly Fault, Sc_m only extends for short distances (< 2 km) into the Northern Sierra terrane and then dies out (Bhattacharyya 1986). In the Sullivan Creek terrane, structures associated with Sc_f are strongly developed only in isolated domains even short distances east of the Melones Fault suggesting that Sc_f did not form penetratively east of this fault. However, it is possible that younger deformations simply reactivated cleavages already present in older rocks. This hypothesis can be examined in regions near the Melones Fault by examining the effects of removing strains present in the eastern Foothills terrane from those measured in the Sullivan Creek terrane. To do so, reciprocal average directed ellipsoids calculated from lapilli tuffs west of the Melones Fault were superimposed on similar ellipsoids east of the fault. For slates the effects of compactions due to volume loss (−48% and −56% for Moccasin and Bagby areas, respectively) were first removed from the average directed ellipsoids for each area. The reciprocal tectonic ellipsoids were then superimposed on total strain ellipsoids obtained from slates east of the fault. Volume losses were not removed from these ellipsoids, since these volume losses preceded or accompanied the development of Sc_m. When this is done, XY planes of the strain ellipsoids and associated cleavages in the Sullivan Creek terrane swing 8-13° counterclockwise to WNW orientations, strain intensities drop slightly and strain types become slightly more prolate (Table 8). These changes are in accord with models proposed for the kinematics of the Melones fault zone (Paterson & Wainger in preparation) and development of conjugate

Table 8. Orientations of strain ellipsoids in the Sullivan Creek terrane after removal of the effects of strains (by multiplying by reciprocal strains) from similar rock types in the eastern Foothills terrane. Note that in most cases strain intensities decrease and *XY* planes move to more WNW orientations

Rock type	Orientation		Strain intensity	Lode's parameter
	X axis	*XY* plane		
Moccasin:				
Lapilli Tuff				
Old ellipsoid	57/310	293/79	1.26	0.32
New ellipsoid	54/294	281/81	1.33	0.14
Slate				
Old ellipsoid	66/85	284/87	1.44	0.42
New ellipsoid	77/83	276/87	1.28	0.33
Virginia Mine:				
Lapilli Tuff				
Old ellipsoid	64/117	308/85	1.12	0.37
New ellipsoid	81/115	297/89	1.02	0.42
Bagby:				
Lapilli Tuff				
Old ellipsoid	82/10	320/84	0.94	0.04
New ellipsoid	77/311	307/89	0.88	−0.33
Slate				
Old ellipsoid	88/64	294/88	1.15	0.71
New ellipsoid	77/83	101/89	0.97	0.34

folds in this region (Paterson in press). Thus, we feel that late Jurassic to early Cretaceous shortening, similar to that which occurred in the eastern Foothills terrane, also occurred in western portions of the Sullivan Creek terrane. Instead of developing new penetrative cleavages, these strains reactivated older cleavages causing an 8–13° clockwise rotation of these structures and only locally developed a new crenulation cleavage.

These observations suggest that in this portion of the Western Metamorphic Belt, Sc_f in the Foothills terrane and Sc_m in the Merced River terrane did not extend much beyond their bounding faults. However, Day *et al.* (1984), Schweickert *et al.* (1984), Varga (1985) and others indicate that this may not be the case in northern parts of the Western Metamorphic Belt. Apparently, Jurassic–Cretaceous cleavages are not restricted to the Foothills terrane, but instead are widespread throughout this portion of the Western Metamorphic Belt (Schweickert *et al.* 1984, Varga 1985).

Rotations of faults and bedding

Most bedding and faults in the region examined display dips steeper than 70°. The only exceptions to this occur in the hinges of gently plunging folds in the Foothills terrane, and near some plutons. Whether or not the steep dips are strictly the result of the strains measured can be determined by using reciprocal strain ellipsoids to determine 'pre-strain' orientations using techniques outlined by Ramsay & Huber (1983). In the western Foothills terrane, bedding now dipping 70° would dip 41° when the reciprocal strain is superimposed, whereas bedding presently dipping 85° would only rotate to 84° dips. Superposition of the less intense strains in the eastern Foothills terrane only rotates beds 5–15°, whereas magnitudes of rotations east of the Melones Fault are similar to those in the western Foothills terrane. Thus, the shortening component of penetrative strain can account for a maximum of 30° of rotation, and in many cases accounts for less than 15° of rotation; either the beds were deformed in such a fashion as to not affect strain markers (e.g. grain-boundary sliding in poorly lithified sediments) or rigid-body rotations of 40°–70° must have occurred throughout these terranes. This does not necessarily imply that the rigid-rotations took place prior to penetrative shortening; the two could have occurred simultaneously. However, several observations indicate that most of the rotations did take place prior to penetrative strain. *Fc* folds are relatively rare throughout the transect. If bedding was horizontal prior to shortening, and penetrative strain occurred simultaneously with rotations, folds should be common. In addition, simultaneous shortening and rotations should result in a variety of strain types (depending on the orientation of compaction ellipsoids with respect to the strain ellipsoids) in the slates and greywackes rather than the widespread flattening strains observed (e.g. Kligfield *et al.* 1981b). As noted earlier this suggestion of early rotations is also supported by an examination of incremental strains measured from quartz fibers near pyrite framboids or crystals. Outside of fault zones these fibers are commonly straight and record strain intensities similar to total strains in greywackes and volcanic rocks measured in the same or nearby samples. The straight fibers indicate that most of the penetrative strains occurred during irrotational deformation after rotation of bedding to steep dips.

Bogen *et al.* (1985) suggested that large rotations occurred across the Melones fault during shortening of the Foothills terrane. Since the walls of shear zones in the Western Metamorphic Belt are strongly shortened, these faults must have formed as reverse faults parallel

to the plane of shortening or rotated towards this plane of flattening, *Sc*, during shortening of the Foothills terrane. Superposition of reciprocal tectonic strains on cleavages in the Melones and Bear Mountains faults suggest that these faults could have formed as E-dipping faults with dips no greater than 50–60° (Paterson & Wainger 1986 and in preparation). If rigid-rotations of these faults also occurred, the faults at one time had rather gentle NE dips.

Shortening of the Western Metamorphic Belt

Estimating the overall change in width of highly deformed rocks is difficult and often impossible to do with any precision (e.g. Schwerdtner 1977). Our studies to date suggest that deformation on a regional-scale was of plane type and that pluton emplacement only locally affects strain fields. If each domain acted as a continuum during deformation (e.g. no discontinuities were present in the domain) and strains were relatively homogeneous, then the averaged directed strains in each domain provide an estimate of the shortening due to penetrative strain for that domain. We have used these strains to estimate minimum values of shortening for the Foothills (42%), Sullivan Creek (53%) and Merced River terranes (60%) along with their 'pre-strain' widths (Table 9).

To progress any further, information is needed about the magnitude of rigid-body rotations in the domains as well as the magnitude of offsets across the faults present between domains (Schwerdtner 1973, 1977). Without a suitable reference frame and/or regional markers, it is difficult to estimate values of rotations. The large rotations implied by the steeply dipping beds, only a part of which can be explained by the intensities of strain measured, indicate that rigid-body rotations did occur along this transect. In addition, the presence of exotic material in, and changes of metamorphic grade across the large ductile shear zones, suggest that large displacements must have occurred across these faults (see also, Sharp 1988). Thus, the magnitudes of shortening obtained from strain data, although significant in themselves, represent minimum values for the overall shortening of the Western Metamorphic Belt.

An increasing number of attempts have been made to use balanced cross-sections in ductilely deformed rocks (Bogen 1984, Woodward *et al.* 1985 and references therein). This study suggests that in metamorphic terranes such an undertaking without a great deal of information about strains, volume losses and timing of rigid-rotations is tenuous at best. The heterogeneous nature of strains, particularly with respect to rock type, the presence of strain discontinuities at lithologic contacts and fault zones, the possibility of orogen-parallel extensions, and variations in strain intensities and orientations along strike, all must be taken into account before such cross-sections can be accurately balanced.

Table 9. Calculated widths of terranes before and after ductile deformation and average values of strain for each domain. These widths do not take into account shortening due to rigid-rotations or faulting and, therefore, represent minimum estimates

Area	Average ductile shortening	Deformed width (km)	Pre-strain width (km)
Western Foothills	55%	8.2	18.22
Central Foothills	40%	6.8	11.33
Eastern Foothills	20%	8.5	10.63
Foothills terrane	42%	23.5	40.18
Sullivan Creek terrane	53%	10.8	22.98
Merced River terrane	60%	15.5	38.75

CONCLUSIONS

Nature of total strains

Total strains associated with regionally developed structures in the Western Metamorphic Belt are heterogeneous and display both regional variations and a strong dependence on rock type. In any one domain, strain intensities are highest in slaty rocks, lower in volcanic rocks, and reach the lowest intensities in greywackes and clast-supported conglomerates. Strain types reflect plane strain in volcanic rocks, whereas large flattening strains occur in slates and greywackes. These flattening strains probably reflect volume losses of −45% to −65% in slates and 0.0 to −26% in greywackes and some pebbly mudstones. If so, then tectonic strains in most domains approach plane to slightly flattening strain types with constrictional strains only developed locally or in regions of complex deformation. Most, if not all, lithologic contacts represent discontinuities in total strain and these discontinuities provide likely locations for the propagation of ductile shear zones.

Number and extent of terranes

We recognize three terranes, the Northern Sierra, Merced River and Foothills terranes, separated by two large ductile shear zones, the Calaveras–Shoo Fly and Melones faults. The Foothills terrane consists of two distinct subterranes, the western and eastern zones, separated by the Bear Mountains Fault and a Mélange zone (Paterson *et al.* 1987a). The similarities in metasedimentary rock types, structures, strains and metamorphism indicate that the Sullivan Creek terrane is a volcanic-rich continuation of the Merced River terrane. If these terrane designations are correct, each of the terranes record a unique structural and metamorphic history and, in the case of the Foothills and Merced River terranes, a unique strain field. Unfortunately, no suitable strain markers were located at this latitude in the Northern Sierra terrane. However, the degree of cleavage development noted in these rock types indicates that strain intensities probably range from near zero in large quartzite blocks to values in excess of those observed elsewhere in the Western Metamorphic Belt. The styles of structure associated with the two earliest deformations in the Northern Sierra

terrane suggest that both were quite strong, but nothing quantitative is known about their relative intensities. Given our present understanding of this terrane, it also displays a unique structural and metamorphic history and strain field.

Two anomalous regions occur in the strain fields from the Foothills and Sullivan Creek terranes. These are the Upper Jurassic volcanic rocks immediately east of the Melones Fault that show very low strains as compared to the rest of the Sullivan Creek terrane, and southern portions of the central Foothills terrane that show anomalously high intensities. Herzig (1985 and personal communication 1986) has noted the presence of sheared serpentinites along the eastern margin of the Upper Jurassic volcanic rocks indicating that these rocks may be large fault-bounded blocks *within* the Melones Fault rather than east of the fault. However, additional work is needed to corroborate this possibility.

South-central portions of the Foothills terrane contain numerous deformed and non-deformed granitoids including the Guadalupe Igneous complex. The anomalously high and often constrictional strains present in this region may reflect local strain fields associated with these granitoids rather than regional patterns, or as noted earlier, complex deformation along the Bear Mountains fault zone.

Terrane boundaries

Each of the terranes and subterranes in the study area is bounded by large ductile fault zones. These zones are the locus of multiple generations of structures (Merguerian 1985, Bhattacharyya 1986, Paterson & Wainger 1986, Paterson *et al.* 1987a, Tobisch & Paterson 1988), and have long and complex movement histories (Clark 1960, Schweickert *et al.* 1982, Paterson *et al.* 1987a). Our strain studies imply that the strains in these faults formed by a combination of simple and pure shear (plus volume losses in phyllosilicate-rich rock types) and that the faults rotated to their present steep dips during shortening of the wallrocks. Schweickert *et al.* (1984) suggested that the Calaveras–Shoo Fly and Melones faults have an east-over-west, or reverse sense of motion. Studies by Paterson & Wainger (1986 and in preparation) indicate the reverse sense of motion for the Melones Fault. The movement in the Bear Mountains Fault is oblique with a dominant east-over-west sense and some sinistral motion (Paterson *et al.* 1987a). No useful kinematic indicators were found in the Calaveras–Shoo Fly thrust.

Models for the structural development of terranes

Tectonic models explaining the genesis of each terrane, and attempts to determine whether or not they are exotic to North America must rest on an integration of geological, geophysical, geochronological and paleomagnetic data. Although such an integration is one of the goals of our ongoing research in this area, such an undertaking is beyond the scope of this paper. However, some mention of the structural constraints on such models seems appropriate.

Our understanding of the nature and timing of deformation is most complete in the Foothills terrane (Paterson & Wainger 1986, Paterson *et al.* 1987a,b, Tobisch *et al.* in press, Saleeby *et al.* in review). Here, the regional cleavage is considered to be late Jurassic to early Cretaceous. Strains associated with this cleavage are highly variable with intensities decreasing from around 1.00 in the western zone to between 0.0 and 0.60 in the eastern Foothills terrane. Assuming 45–65% deviatoric volume reductions in slaty rocks, values of penetrative tectonic shortening range from around 50% in the western Foothills to 0–30% in the eastern Foothills indicating a minimum shortening of 42% for the Foothills terrane. In most domains, bulk strains reflect plane strain, but in some slates and parts of the central and eastern Foothills terrane, a small orogen-parallel extension occurred. Directions of greatest extension usually plunge steeply in the western Foothills but gradually shallow to the east, whereas steep-dipping XY planes of strain change from 320° strikes in the east to 331° strikes in the west.

An integration of structures with total and incremental strains suggests that deformation in the Foothills terrane involved early rigid-body rotations of bedding and faults with subsequent ductile shortening. Age dates on deformed plutons, as well as structural studies, indicate that the Melones and Bear Mountains fault zones were active during the early rigid-body rotations as well as the later ductile shortening (Tobisch *et al.* in press, Paterson & Wainger in preparation). These faults may have originated as northeast-dipping thrusts, and rotated to their present steep dips during shortening of the wallrocks, or as steep E-dipping reverse faults. Notably absent in this portion of the Foothills terrane is any evidence for large E-directed thrusts noted by Day *et al.* (1984) in the northern Sierra. If present, such structures must be preserved in basement rocks, or rotated to steep dips and strongly overprinted by the structures described herein. Structures associated with the ductile deformation of the Foothills terrane are not common in the study area east of the Melones fault but may be represented by small domains of crenulation cleavage, rare conjugate folds (Paterson in press), and by the clockwise rotation of older structures in the Sullivan Creek terrane (Table 8).

Varga (1985), using the style and orientation of structures, argued that late Jurassic structures in the northern Sierra Nevada formed during orthogonal plate convergence. If such structures do reflect plate motions, this study indicates that late Jurassic structures formed during orthogonal convergence, but that ductile structures younger than 150 Ma reflect oblique convergence. This late, oblique convergence is suggested by (1) oblique (southeast-over-north) motion on the Bear Mountains Fault (Paterson *et al.* 1987a), (2) common SE-plunging stretching lineations and fold axes in the Foothills terrane, (3) a small amount of late sinistral movement in the Melones Fault (Paterson & Wainger in preparation) and

(4) NW–SE directions of shortening calculated from rare kink folds (Paterson in press). This change from orthogonal to oblique convergence at *ca* 150 Ma agrees remarkably well with the change in plate motions suggested by May & Butler (1986).

In the Merced River and Sullivan Creek terranes, the regional cleavage is *ca* 177 Ma old (Sharp 1983, 1985) and younger domainal structures late Jurassic or younger (Schweickert *et al.* 1984, Paterson in press). Minimum values of tectonic shortening associated with the older regional cleavage fall between 50 and 60% with directions of greatest extension plunging steeply. Assuming deviatoric volume losses of 45–65% for phyllites, tectonic strains are of plane to flattening types, with small regions of constrictional strain possibly representing areas of 'return flow'. Estimates of 0–35% shortening associated with the younger domainal structures have been noted by Paterson (in press). Minimum values of tectonic shortening for the Sullivan Creek and Merced River terranes are 53% and 60% respectively (Table 9).

We have not been able to constrain the kinematics of deformation as well in these terranes, but some combination of rigid-rotations, faulting and ductile shortening must have occurred. The WNW strikes of cleavage, steeply plunging stretching lineations, and associated large strains indicate that a major period of NNE–SSW tectonic shortening (plate motion?) occurred prior to the late Jurassic orthogonal convergence noted above (see also Sharp 1988). The chaotic distribution of rock types in this terrane and widespread olistostromal deposits have suggested to many workers that some of the early structures probably formed before the rocks were completely lithified (Schweickert *et al.* 1977, Bhattacharyya 1986, Sharp 1988). A comparison of the Merced River terrane to a modern accretionary wedge has led Paterson & Sample (1988) to suggest that most of the pre-late Jurassic structures in this terrane developed by underplating at deeper levels in an accretionary complex.

In summary, we wish to emphasize the heterogenous nature and causes of structures and associated strains developed in lithologically complex terranes. The total strains examined in this study reflect variations in primary fabrics, volume losses, and lithologically controlled partitioning of tectonic strains. Although these strains and associated structures may ultimately be related to plate motions, we feel they are more usefully viewed as reflecting the behavior of a lithologically complex sequence of rocks deformed in diverse tectonic settings and conditions.

Acknowledgements—This work was supported by National Science Foundation Grants EAR 8318212 and 8503882. We would like to thank Sam Longiaru for writing many of the computer programs used in this study and for comments made about the manuscript. We also thank Dr Gerhard Oertel for use of the X-ray pole-figure goniometer at UCLA, advice and help while completing analyses of the slates, and for comments made about the manuscript. We thank Lisa Wainger, Judi Radloff and Tim Redfield for help in obtaining strain data. Scott Paterson would like to thank his friend Margie Whalen for her love and support during the tenure of this project. We thank Peter Hudleston and an anonymous reviewer for comments about the manuscript. Many other people spent time talking about the geology of the Sierra Nevada or methods for measuring strains and we thank them for these discussions.

REFERENCES

Bateman, P. C., Harris, A. G., Kistler, R. W. & Krauskopf, K. B. 1985. Calaveras reversed: westward younging is indicated. *Geology* **13**, 338–341.

Behrman, P. H. 1979. Features of the Melones Fault zone, central Sierra Nevada foothills, California. *Geol. Soc. Am. Abs. w. Prog.* **11**, 58.

Bell, T. H., Fleming, P. D. & Rubenach, M. J. 1986. Porphyroblast nucleation, growth and dissolution in regional metamorphic rocks as a function of deformation partitioning during foliation development. *J. Metam. Geol.* **4**, 37–67.

Best, M. 1963. Petrology and structural analysis of metamorphic rocks in the southwestern Sierra Nevada Foothills. *California Univ. Publs. Geol. Sci.* **42**, 111–157.

Beutner, E. C. & Diegel, F. A. 1985. Determination of fold kinematics from syntectonic fibers in pressure shadows, Martinsburg Slate, N. J. *Am. J. Sci.* **285**, 16–50.

Bhattacharyya, T. 1986. Tectonic evolution of the Shoo Fly formation and the Calaveras complex, central Sierra Nevada, California. Unpublished Ph.D. dissertation, University of California, Santa Cruz.

Bhattacharyya T. & Paterson, S. R. 1985. Discussion of timing and structural expression of the Nevadan orogeny, Sierra Nevada, California. *Bull. geol. Soc. Am.* **96**, 1346–1347.

Blake, M. C., Jr, Howell, D. G. & Jones, D. L. 1982. Preliminary tectonostratigraphic terrane map of California. *U. S. Geol. Surv. Open-File Report* **82**, 593.

Bogen, N. 1983. Studies of the Jurassic Geology of the west-central Sierra Nevada of California. Unpublished Ph.D dissertation, Columbia University.

Bogen, N. L. 1984. Stratigraphic and sedimentologic evidence of a submarine island-arc volcano in the lower Mesozoic Penon Blanco and Jasper Point Formations, Mariposa County, California. *Bull. geol. Soc. Am.* **96**, 1322–1331.

Bogen, N. L., Kent, D.V. & Schweickert, R. A. 1985. Paleomagnetic constraints on the structural development of the Melones and Sonora faults, central Sierran foothills, California. *J. geophys. Res.* **90**, 4627–4636.

Boulter, C. A. 1986. Strain paths during slaty cleavage formation–the role of volume loss: Discussion. *J. Struct. Geol.* **8**, 719–720.

Castro, A. 1986. Structural pattern and ascent model in the Central Extremadura batholith, Hercynian belt, Spain. *J. Struct. Geol.* **8**, 633–646.

Clark, L. D. 1960. Foothills fault system, western Sierra Nevada California. *Bull. geol. Soc. Am.* **71**, 483–496.

Clark, L. D. 1964. Stratigraphy and structure of part of the western Sierra Nevada metamorphic belt, California. *Prof. Pap. U. S. Geol. Surv.* **410.**

Cobbold, P. R. 1977. Description and origin of banded deformation structures. I. Regional strain, local perturbations, and deformation bands. *Can. J. Earth Sci.* **14**, 1721–1731.

Coward, M. P. & Kim, J. H. 1981. Strain within thrust sheets. In: *Thrust and Nappe Tectonics* (edited by McClay, K. R. & Price, N. J.). *Spec. Publ. geol. Soc. Lond.* **9**,275–292.

Davison, I. 1987. Normal fault geometry related to sediment compaction and burial. *J. Struct. Geol.* **9**, 393–402.

Day, H. W., Moores, E. M. & Tuminus, A. C. 1984. Structure and tectonics of the northern Sierra Nevada. *Bull. geol. Soc. Am.* **96**, 436–450.

Day, H. W., Schiffman, P. & Moores, E. M. 1986. Regional metamorphism and tectonics of the northern Sierra Nevada, California. *Geol. Soc. Am. Abs. w. Prog.* **18**, 582.

Ehrreich, A. L. 1965. Metamorphism, migmatites, and intrusion in the Foothills of the Sierra Nevada, Madera, Mariposa, and Merced Counties, California. Unpublished Ph.D. dissertation, University of California, Los Angeles.

Ellis, M. A. 1986. The determination of progressive deformation histories from antitaxial syntectonic crystal fibers. *J. Struct. Geol.* **8**, 701–709.

Engelder, T. & Oertel, G. 1985. Correlation between abnormal pore pressure and tectonic jointing in the Devonian Catskill delta. *Geology* **13**, 863–866.

Freeman, B. 1987. The behavior of deformable ellipsoidal particles in three-dimensional slow flows: implications for geological strain analyses. *Tectonophysics* **132**, 297–309.

Gay, N. C. 1976. The change in shape of a viscous ellipsoidal region embedded in a slowly deforming matrix having a different viscosity — A discussion. *Tectonophysics* **35**, 403–409.

Herzig, C. T. 1985. Jurassic rocks east of the Melones fault zone, central Sierra Nevada foothills, California. Unpublished Master thesis, State University of New York, Stony Brook.

Hossack, J. R. 1968. Pebble deformation and thrusting in the Bygdin area (S. Norway). *Tectonophysics* **5**, 315–339.

Kligfield, R., Carmignani, L. & Owens, W. H. 1981a. Strain analyses of a northern Apennine shear zone using deformed marble breccias. *J. Struct. Geol.* **3**, 421–436.

Kligfield, R., Owens, W. H. & Lowrie, W. 1981b. Magnetic susceptability anisotropy, strain, and progressive deformation in Permian sediments from the Maritime Alps (France). *Earth Planet. Sci. Lett.* **55**, 181–189.

Krauskopf, K. B. 1985. Geologic map of the Mariposa quadrangle, Mariposa and Madera counties, California. *U. S. Geol. Survey Map* GQ–1586.

Lisle, R. J. 1977. Clastic grain shape and orientation in relation to cleavage from Aberystwyth grits, Wales. *Tectonophysics* **12**, 307–325.

Mannion, L. E. 1960. Geology of the La Grange Quadrangle. Unpublished Ph.D. dissertation, Stanford University.

May, S. R. & Butler, R. F. 1986. North American Jurassic apparent polar wander: Implications for plate motion, paleogeography and Cordilleran tectonics. *J. geophys. Res.* **91**, 11,519–11,544.

Merguerian C. 1982. The extension of the Calaveras–Shoo Fly Thrust (CSFT) to the southern end of the Sierra Nevada Metamorphic Belt (SNMB), California. *Geol. Soc. Am. Abs. w. Prog.* **14**, 215.

Merguerian, C. 1985. Tectonic significance of mylonitic Paleozoic gneissic granitoids in the Shoo Fly complex, Toulumne county, California. *Geol. Soc. Am. Abs. w. Prog.* **17**, 369.

Miller, D. M. & Oertel, G. 1979. Strain determination from the measurement of pebble shapes: a modification. *Tectonophysics* **55**, T11–T13.

Nokleberg, W. J. 1983. Wall rocks of central Sierra Nevada Batholith, California: a collage of tectonostratigraphic terranes accreted in Alaska–type arc settings. *Prof. Pap. U. S. Geol. Surv.* **1255**.

Oertel, G. 1970. Deformation of a slaty lapillar tuff in the Lake District, England. *Bull. geol. Soc. Am.* **81**, 1173–1188.

Oertel, G. 1981. Strain estimation from scattered observations in an inhomogeneously deformed domain of rocks. *Tectonophysics* **77**, 133–150.

Paterson, S. R. 1986. Strains, metamorphism, and structural evolution of tectonostratigraphic terranes in the Western Metamorphic belt, Sierra Nevada, California. Unpublished Ph.D. dissertation, University of California at Santa Cruz.

Paterson, S. R. In press. A reinterpretation of conjugate folds in the central Sierra Nevada, California. *Bull. geol. Soc. Am.*

Paterson, S. R. & Redfield, T. F. 1984. Finite strains and associated structures across the Melones fault zone near Moccasin, California. *Geol. Soc. Am. Abs. w. Prog.* **16**, 619.

Paterson, S. R. & Sample, J. C. 1988. The development of folds and cleavages in slate belts by underplating in accretionary complexes: a comparison of the Kodiak Formation, Alaska and the Calaveras Complex, California. *Tectonics* **7**, 859–874.

Paterson, S. R., Tobisch, O. T. & Radloff, J. K. 1987a. Post-Nevadan deformation along the Bear Montains fault zone: implications for the Foothills terrane, central Sierra Nevada, California. *Geology* **15**, 513–516.

Paterson, S. R., Tobisch, O. T. & Saleeby, J. B. 1987b. Recognition of pretectonic intrusives: implications for the dating of structural events. *Geol. Soc. Am. Abs. w. Prog.* **19**, 800.

Paterson, S. R. & Wainger, L. 1986. Variations of structures and strains in the southern Melones fault zone, Sierra Nevada, California. *Geol. Soc. Am. Abs. w. Prog.* **18**, 169.

Ramsay, J. G. 1982. Rock ductility and its influence on the development of tectonic structures in mountain belts. In: *Mountain Building Processes* (edited by Hsu, K.). Academic Press, London, 111–127.

Ramsay, J. G. & Huber, M. I. 1983. *The Techniques of Modern Structural Geology Volume 1: Strain Analysis.* Academic Press, London, 111–127.

Saleeby, J. B. 1981. Ocean floor accretion and volcanoplutonic arc evolution of the Mesozoic Sierra Nevada. In: *The Geotectonic Development of California* (edited by Ernst, W. G.), 132–181.

Saleeby, J. B. 1982. Polygenetic ophiolite belt of the California Sierra Nevada: Geochronological and tectonostratigraphic development. *J. geophys. Res.* **87**, 1803–1824.

Sanderson, D. J. 1976. The superposition of compaction and plane strain. *Tectonophysics* **30**, 35–54.

Schweickert, R. A. 1981. Tectonic evolution of the Sierra Nevada Range, In: *The Tectonic Development of California* (edited by Ernst, W. G.), 87–131.

Schweickert, R. A. & Bogen, N. L. 1983. Tectonic transect of Sierran Paleozoic through Jurassic accreted belts. *Pacific Sec. Soc. Econ. Paleon. and Mineral.* Field Guide.

Schweickert, R. A., Bogen, N. L. & Engelder, J. T. 1982. Structural history of the Melones fault zone, western Sierra Nevada, California. *Geol. Soc. Am. Abs. w. Prog.* **14**, 231–232.

Schweickert, R. A., Bogen, N. L., Girty, G. H., Hanson, R. A. & Merguerian, C. 1984. Timing and structural expression of the Nevadan orogeny, Sierra Nevada, California. *Bull. geol. Soc. Am.* **95**, 967–979.

Schweickert, R. A., Bogen, N. L., Girty, G. H., Hanson, R. E. & Merguerian, C. 1985. Timing and structural expression of the Nevadan orogeny, Sierra Nevada, California: Discussion and reply. *Bull. geol. Soc. Am.* **96**, 1346–1352.

Schweickert, R. A., Saleeby, J. B., Tobisch, O. T. & Wright, W. H. 1977. Paleotectonic and paleogeographic significance of the Calaveras Complex western Sierra Nevada, California. In: *Paleozoic Paleogeography of the Western United States* (edited by Stewart, J. H., Stevens, C. H. & Fritsche, A. E.). *Pacific Sec. Soc. Econ. Paleon. and Mineral. Sym.* **1**, 381–394.

Schwerdtner, W. M. 1973. A scale problem in paleo-strain analysis. *Tectonophysics* **16**, 47–54.

Schwerdtner, W. M. 1977. Geometric interpretation of regional strain analyses. *Tectonophysics* **39**, 515–531.

Schwerdtner, W. M., Bennett, P. J. & Janes, W. T. 1977. Application of L–S fabric scheme to structural mapping and paleostrain analysis. *Can. J. Earth. Sci.* **14**, 1021–1032.

Sharp, W. D. 1983. Chronology of the structural development of the central Sierra Nevada Foothills, California. *Geol. Soc. Am. Abs. w. Prog.* **15**, 272.

Sharp, W. D. 1985. The Nevadan orogeny of the Foothills metamorphic belt, California: a collision without a suture? *Geol. Soc. Am. Abs. w. Prog.* **17**, 407.

Sharp, W. D. 1988. Pre-Cretaceous crustal evolution in the Sierra Nevada region, California. In: *Metamorphism and Crustal Evolution of the Western United States* (edited by Ernst, W. G.). Prentice-Hall, New York.

Sharp, W. D., Saleeby, J., Schweickert, R., Merguerian, C., Kistler, R., Tobisch, O. & Wright, W. H. 1982. Age and tectonic significance of Paleozoic orthogneisses of the Sierra Nevada foothills metamorphic belt. *Geol. Soc. Am. Abs. w. Prog.* **14**, 233.

Shimamoto, I. & Ikeda, Y. 1976. A simple algebraic method for strain estimation from deformed ellipsoidal objects. 1. Basic theory. *Tectonophysics* **36**, 315–337.

Tobisch, O. T. & Paterson, S. R. 1988. Analysis and interpretation of composite foliations in areas of progressive deformation. *J. Struct. Geol.* **10**, 745–754.

Tobisch, O. T., Paterson, S. R., Longiaru, S. & Bhattacharyya, T. 1987. Extent of the Nevadan orogeny, central Sierra Nevada, California. *Geology* **15**, 132–135.

Tobisch, O. T., Paterson, S. R., Saleeby, J. B. & Geary, E. E. In press. Nature and timing of deformation in the Foothills terrane, Central Sierra Nevada, California: implications for orogenesis. *Bull. geol. Soc. Am.* **101**.
1987. Extent of the Nevadan orogeny, central Sierra Nevada, California. *Geology* **15**, 132–135.

Treagus, S. H. 1983. A theory of finite strain variation through contrasting layers, and its bearing on cleavage refraction. *J. Struct. Geol.* **5**, 351–368.

Tullis, T. E. & Wood, D. S. 1975. Correlation of finite strain from both reduction bodies and preferred orientation of mica in slate from Wales. *Bull. geol. Soc. Am.* **86**, 632–638.

Varga, R. J. 1985. Mesoscopic structural fabric of early Paleozoic rocks in the northern Sierra Nevada, California and implications for Late Jurassic plate kinematics. *J. Struct. Geol.* **7**, 667–682.

Wheeler, J. 1986. Strain analysis in rocks with pretectonic fabrics. *J. Struct. Geol.* **7**, 667–682.

Wright, O. T. & Platt, L. B. 1982. Pressure dissolution and cleavage in the Martinsburg shale. *Am. J. Sci.* **282**, 122–135.

Woodward, N. B., Boyer, S. E. & Suppe, J. 1985. An outline of balanced cross-sections. *Short Course Outline. geol. Soc. Am.*